



**UvA-DARE (Digital Academic Repository)**

**Experimental test of the interlayer pairing models for high-T<sub>c</sub> superconductors using grazing-incidence infrared reflectometry**

Schuetzmann, J.; Somal, H.S.; Tsvetkov, A.A.; van der Marel, D.; Koops, G.E.J.; Kolesnikov, N.; Ren, Z.F.; Wang, J.H.; Bruck, E.H.; Menovsky, A.A.

*Published in:*

Physical Review. B, Condensed Matter

*DOI:*

[10.1103/PhysRevB.55.11118](https://doi.org/10.1103/PhysRevB.55.11118)

[Link to publication](#)

*Citation for published version (APA):*

Schuetzmann, J., Somal, H. S., Tsvetkov, A. A., van der Marel, D., Koops, G. E. J., Kolesnikov, N., ... Menovsky, A. A. (1997). Experimental test of the interlayer pairing models for high-T<sub>c</sub> superconductors using grazing-incidence infrared reflectometry. *Physical Review. B, Condensed Matter*, 55, 11118-11121. DOI: 10.1103/PhysRevB.55.11118

**General rights**

It is not permitted to download or to forward/distribute the text or part of it without the consent of the author(s) and/or copyright holder(s), other than for strictly personal, individual use, unless the work is under an open content license (like Creative Commons).

**Disclaimer/Complaints regulations**

If you believe that digital publication of certain material infringes any of your rights or (privacy) interests, please let the Library know, stating your reasons. In case of a legitimate complaint, the Library will make the material inaccessible and/or remove it from the website. Please Ask the Library: <http://uba.uva.nl/en/contact>, or a letter to: Library of the University of Amsterdam, Secretariat, Singel 425, 1012 WP Amsterdam, The Netherlands. You will be contacted as soon as possible.

## Experimental test of the interlayer pairing models for high- $T_c$ superconductivity using grazing-incidence infrared reflectometry

J. Schützmann, H. S. Somal, A. A. Tsvetkov,\* D. van der Marel, and G. E. J. Koops  
Materials Science Centre, Laboratory of Solid State Physics, University of Groningen,  
Nijenborgh 4, 9747 AG Groningen, The Netherlands

N. Koleshnikov  
Institute of Solid State Physics, Russian Academy of Sciences, Chernogolovka, 142432 Russia

Z. F. Ren and J. H. Wang  
Department of Chemistry, SUNY at Buffalo, Buffalo, New York 14260-3000

E. Brück and A. A. Menovsky  
Van der Waals-Zeeman Institute, University of Amsterdam, The Netherlands  
(Received 21 January 1997)

From measurements of the far-infrared reflectivity at grazing angles of incidence with  $p$ -polarized light we determined the  $c$ -axis Josephson plasma frequencies of the single layer high- $T_c$  cuprates  $Tl_2Ba_2CuO_6$  and  $La_{2-x}Sr_xCuO_4$ . We detected a strong plasma resonance at  $50\text{ cm}^{-1}$  for  $La_{2-x}Sr_xCuO_4$  in excellent agreement with previously published results. For  $Tl_2Ba_2CuO_6$  we were able to determine an upper limit of the unscreened  $c$ -axis Josephson plasma frequency  $100\text{ cm}^{-1}$  or a  $c$ -axis penetration depth  $>15\text{ }\mu\text{m}$ . The small value of  $\omega_J$  stands in contrast to recent a prediction based on the interlayer tunneling mechanism of superconductivity. [S0163-1829(97)00818-7]

A striking feature of the high- $T_c$  cuprates is the strong anisotropy of the conductivity. Both the low conductivity in the  $c$  direction (below the Mott limit) and the frequency dependence (no Drude peak) support the ‘‘confinement’’ hypothesis<sup>1</sup> stating that hopping of single electrons between neighboring  $CuO_2$  planes is inhibited in the normal state due to spin-charge separation. As tunneling of pairs of carriers is still allowed, the formation of Cooper pairs results in a gain of kinetic energy, which stabilizes the superconducting state. Therefore within the Chakravarty-Anderson interlayer model the main contribution to the condensation energy ( $E_{\text{cond}}$ ) is due to the Josephson coupling between adjacent  $CuO_2$  planes. Recently Anderson<sup>2</sup> pointed out that, since the Josephson coupling energy is proportional to the plasma frequency of the condensate ( $\omega_J$ ), a proportionality should exist between  $\omega_J$  and  $T_c$  for the cuprates with one  $CuO_2$  layer per unit cell. One of the best compounds for testing the confinement hypothesis appears to be  $Tl_2Ba_2CuO_y$  at optimal oxygen concentration due to its high value of  $T_c$  (85 K) and the large separation between  $CuO_2$  planes ( $11.57\text{ }\text{Å}$ ). According to the interlayer tunneling (ILT) hypothesis<sup>2-4</sup>

$$\hbar^2\omega_J^2 = \eta E_{\text{cond}} \frac{16\pi d e^2}{a^2}, \quad (1)$$

where  $\eta$  represents the fraction of the condensation energy contributed by the ILT mechanism,<sup>4</sup>  $d$  is the spacing between adjacent  $CuO_2$  planes, and  $a$  is the in-plane lattice parameter. The condensation energy ( $E_{\text{cond}} \propto T_c^2$ ) can be obtained directly from the specific heat,<sup>5</sup> resulting in  $E_{\text{cond}} = 80\text{ }\mu\text{eV}$  per unit of  $CuO_2$  for  $Tl_2Ba_2CuO_y$  ( $T_c = 85\text{ K}$ ) and  $13\text{ }\mu\text{eV}$  for slightly underdoped  $La_{2-x}Sr_xCuO_4$  ( $T_c = 32\text{ K}$ ). The

above expression for  $\omega_J$  is radically different from conventional BCS theory, where, adopting a ‘‘dirty-limit’’ scenario for the  $c$ -axis conductivity,  $\omega_J^2$  follows from the Glover-Tinkham-Ferrel sum rule<sup>6</sup>

$$\hbar^2\omega_J^2 = 4\pi^2\hbar\sigma_n\Delta(0). \quad (2)$$

Using the ILT prediction [Eq. (1)] we calculate that  $\omega_J \approx 1500\text{ cm}^{-1}$  for  $Tl_2Ba_2CuO_y$  and  $530\text{ cm}^{-1}$  for  $La_{2-x}Sr_xCuO_4$  ( $T_c = 32\text{ K}$ ). In contrast, using Eq. (2) we calculate  $\omega_J \approx 200\text{ cm}^{-1}$  and  $230\text{ cm}^{-1}$  for  $Tl_2Ba_2CuO_y$  and  $La_{2-x}Sr_xCuO_4$ , respectively. These values for  $\omega_J$  should still be complemented with the atomic polarizabilities and optical-phonon parameters for each of these compounds to obtain the full  $c$ -axis dielectric function

$$\epsilon_c = \epsilon_\infty - \frac{\omega_J^2}{\omega^2} + \frac{4\pi i}{\omega} \sigma_e + \sum_j \frac{S_j \omega_j^2}{\omega_j^2 - \omega(\omega + i/\tau_j)}, \quad (3)$$

from which follows the position of the screened Josephson plasma resonance.

Most experimental techniques aimed at measuring the  $c$ -axis penetration depth or  $\omega_J$  require single crystals of sufficient thickness (several mm) in the  $c$  direction. Lacking large crystals of  $Tl_2Ba_2CuO_6$  we adopted a different approach: By measuring the intensities of  $p$ -polarized light reflected from the  $ab$  surface at a grazing angle of incidence ( $80^\circ$ ) we can probe the longitudinal optical modes for the electric-field vector along the  $c$  axis including the  $c$ -axis Josephson plasmon. In this study we used several flux-grown  $Tl_2Ba_2CuO_6$  single crystals from the same batch.<sup>7</sup> The typical size of the crystals is  $2 \times 2\text{ mm}$  in the  $ab$  plane and  $0.1$

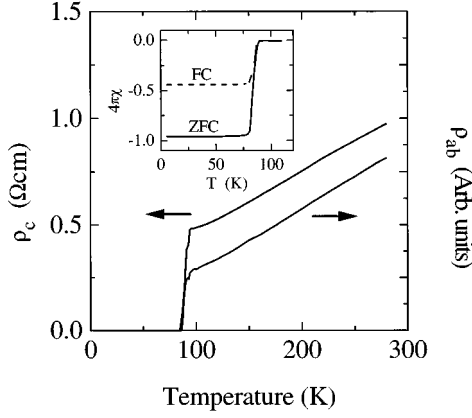


FIG. 1. dc resistivity and dc susceptibility measured with  $H||ab$  (10 Oe) of a  $Tl_2Ba_2CuO_6$  single crystal.

mm along the  $c$  direction. The field-cooled and zero-field cooled dc magnetic susceptibility (inset of Fig. 1) shows a 10-K wide transition with an onset at 90 K. For the dc transport measurements four gold contacts were evaporated, followed by a mild baking at 250 °C. The arrangement of the four voltage and current contacts was selected for obtaining an accurate value of  $\rho_c$ , but only relative changes of  $\rho_{ab}$  could be obtained. Both  $\rho_c$  and  $\rho_{ab}$  have a linear temperature dependence (Fig. 1) as has been reported before for this compound by a number of groups.<sup>8</sup> The drop in resistivity takes place between 95 and 85 K. Details about the preparation and characterization of the  $Tl_2Ba_2CuO_6$  films ( $T_c = 80$  K) and of the  $La_{2-x}Sr_xCuO_4$  crystals were described in Refs. 9 and 10, respectively.

For a strongly anisotropic material with a high conductivity in the  $ab$  plane and a low conductivity along the  $c$  axis, minima are found in the reflectivity

$$R_p = \left| \frac{Z_0 - Z_s^p}{Z_0 + Z_s^p} \right|^2 \quad (4)$$

when  $\text{Re}Z_s^p$  has a maximum. Here  $Z_0$  is the vacuum impedance. The surface impedance for  $p$ -polarized light at oblique incidence is

$$Z_s^p = \frac{Z_0}{n_{ab} \cos \theta} \sqrt{1 - \frac{\sin^2 \theta}{\epsilon_c}} \quad (5)$$

where  $\theta$  is the angle of incidence with the surface normal, and  $n_{ab}^2 = \epsilon_{ab}$  is the  $ab$ -plane component of the dielectric tensor. The  $c$ -axis longitudinal modes appear as sharp resonances in the surface resistance,<sup>11</sup> which is proportional to the pseudoloss function

$$L(\omega) = \text{Im} e^{i\phi} \frac{\sqrt{1 - (\sin^2 \theta / \epsilon_c)}}{1 + |Z_s^p / Z_0|^2} = \frac{(1 - R_p) |n_{ab}| \cos \theta}{2(1 + R_p)}. \quad (6)$$

$L(\omega)$  is roughly the same as the  $c$ -axis loss function  $\text{Im}(-1/\epsilon_c)$  apart from a weakly frequency-dependent phase shift  $\phi = \pi/2 - \arg(n_{ab})$ . The second equality in Eq. (6) can be used to calculate  $L(\omega)$  from the grazing incidence reflectivity data. Although this requires an estimate of  $|n_{ab}|$ , as  $|n_{ab}|$  has a smooth frequency dependence, the multiplication

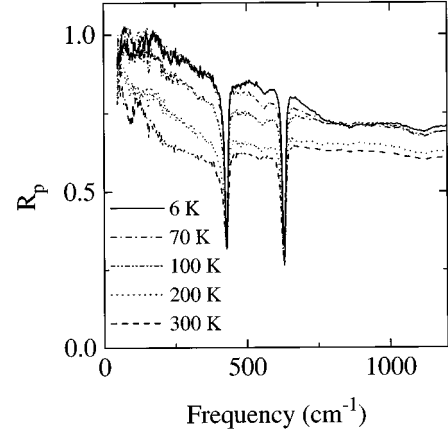


FIG. 2. Reflectivity  $R_p$  of a  $Tl_2Ba_2CuO_6$  single crystal measured with  $p$ -polarized light incident on the  $ab$  surface at an angle of 80°.

with this factor does not influence the position and line shape of the  $c$ -axis longitudinal modes.

The  $p$ -polarized reflectivity was measured at an angle of incidence of  $\theta = 80^\circ$ . To increase the probing area, we mounted a mosaic of four crystals which was fixed on top of a cone in order to reject stray light. Absolute reflectivities were obtained by referencing the intensity reflected from the samples to the reflectivity after Au coating the samples *in situ*. In Fig. 2 we present the grazing incidence reflectivity of the  $Tl_2Ba_2CuO_{6+\delta}$  crystal.  $R_p$  is characterized by a strong increase with decreasing temperature, which is caused by the temperature dependence of the in-plane optical conductivity. For  $T = 6$  K we observe deep and narrow minima<sup>12</sup> at 157, 429, 631  $cm^{-1}$ , which lie close to the out-of plane frequencies (143, 451, and 648  $cm^{-1}$ ) obtained from lattice-dynamical calculations.<sup>13</sup> Surprisingly an LO apex-oxygen bending mode predicted at 348  $cm^{-1}$  with a relatively large oscillator strength is absent in our data, similar to what was observed for  $Tl_2Ba_2Ca_2Cu_3O_{10}$ .<sup>14</sup> From Eq. (3) we see, that the half-width of the LO phonons in the loss function ( $\text{Im}1/\epsilon_c$ ) is given by  $1/\tau + 4\pi\sigma_e\epsilon_\infty^{-1}S/(\epsilon_\infty + S)$ , where  $\tau$  is the intrinsic phonon lifetime,  $S$  is the oscillator strength, and  $\sigma_e$  is the electronic optical conductivity. Hence the width of these peaks can be used to estimate  $\sigma_e$ . After correcting for peak asymmetries of the pseudoloss function introduced through the phaseshift  $\phi$ , we obtained that  $\sigma_e = 0.7 \pm 0.3$  S/cm near 500  $cm^{-1}$ , i.e., below the dc conductivity at 100 K (2 S/cm). Two strongly damped modes at 86 and 538  $cm^{-1}$  are close to the calculated in-plane mode frequencies (84 and 560  $cm^{-1}$ ). Having established these best-fit parameters for the optical phonons we were able to determine the electronic contribution of the in-plane optical conductivity by fitting the experimental data over a wide frequency range (50 – 6000  $cm^{-1}$ ) to Eq. (4). Our estimated in-plane optical conductivity is in excellent agreement with recent results by Puchkov *et al.*<sup>15</sup>

Although in the normal state the free-carrier  $c$ -axis plasmon is known to be overdamped in the cuprates, in the superconducting state we expect to observe a plasma minimum in  $R_p$  at the screened plasma resonance  $\omega_{ps}/\sqrt{\epsilon_S}$ ,<sup>16</sup> where  $\epsilon_S$  is the background dielectric function [see Eq. (3)]. To demonstrate the reliability of the grazing incidence method

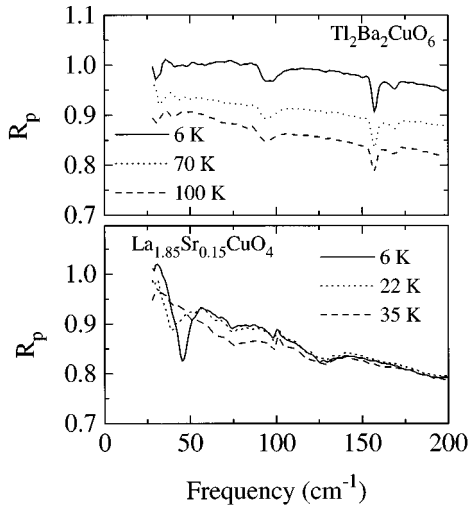


FIG. 3. Reflectivity  $R_p$  of a  $\text{Tl}_2\text{Ba}_2\text{CuO}_6$  thin film (upper panel) and of a  $\text{La}_{1.85}\text{Sr}_{0.15}\text{CuO}_4$  single crystal measured with  $p$ -polarized light incident on the  $ab$  surface at an angle of  $80^\circ$ .

we display in the lower part of Fig. 3  $R_p$  measured on the  $ab$  plane of a  $\text{La}_{2-x}\text{Sr}_x\text{CuO}_4$  single crystal. Below  $T_c$  a minimum occurs, which sharpens and shifts to  $50 \text{ cm}^{-1}$  upon reducing temperature, consistent with the temperature dependence of  $\omega_J$  found from normal incidence reflectivity measurements<sup>17</sup> on the  $ac$  plane of this crystal. Such a structure is not present in the far-infrared or mid-infrared reflectivity spectra for the  $\text{Tl}_2\text{Ba}_2\text{CuO}_6$  single crystal (Fig. 2) in the measured frequency range. Since at low frequencies the signal-to-noise ratio is limited by the small size of the crystals, we also measured  $R_p$  of thin films of  $\text{Tl}_2\text{Ba}_2\text{CuO}_6$  in the frequency range from 20 to  $8000 \text{ cm}^{-1}$ . We observed the same overall behavior and optical phonon spectrum as for the single crystal except for an additional optical phonon of the  $\text{SrTiO}_3$  substrate at  $170 \text{ cm}^{-1}$ . The reflectivity is shown on an expanded scale in the upper panel of Fig. 3. Even with the strongly improved signal-to-noise ratio no clear evidence for a Josephson plasmon is present in these data, except perhaps for a rather broad and shallow minimum at  $40 \text{ cm}^{-1}$ .

To enable a direct comparison to theory, we display in Fig. 4(a) the  $c$ -axis pseudoloss function for  $\text{Tl}_2\text{Ba}_2\text{CuO}_6$ , both in the normal and in the superconducting state, calculated from the reflectivity spectra (Fig. 2) using Eq. (6), while adopting a smoothly frequency-dependent  $ab$ -plane dielectric function  $\epsilon_{ab}$  fitted to  $R_p$  over a wide frequency range up to  $8000 \text{ cm}^{-1}$ . In Figs. 4(b)–4(d) we display model calculations of the pseudoloss function based on the two scenario's (BCS and ILT) outlined in the Introduction. We used the optical-phonon parameters discussed above.<sup>12</sup> The phase shift  $\phi$  was calculated from the in-plane dielectric function mentioned above. In Figs. 4(c) and 4(d) the superconducting response was calculated with a Josephson plasma frequency calculated from the BCS expression [Eq. (2)]. In Fig. 4(c) it was assumed that there is no residual  $c$ -axis optical conductivity at the position of the Josephson plasma resonance ( $50 \text{ cm}^{-1}$ ). In Fig. 4(d) a small residual conductivity of  $3 \text{ S/cm}$  was added near the resonance. Such a residual conductivity is expected in the case of  $d$ -wave pairing in the presence of impurity scattering. We notice that the occurrence of the Josephson plasmon at  $50 \text{ cm}^{-1}$  has no noticeable effect on the

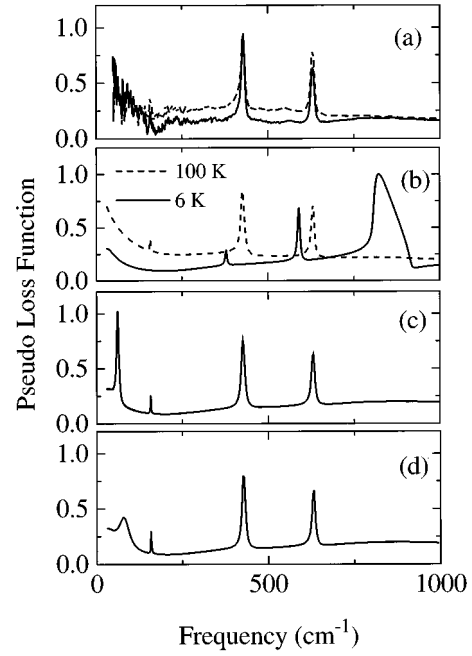


FIG. 4. Pseudoloss function  $L(\omega)$  of  $\text{Tl}_2\text{Ba}_2\text{CuO}_6$ : (a) experimental data at 100 K (dashed curve) and 6 K (solid), (b) simulation for the normal state (dashed) and for the superconducting state (solid) adopting the ILT value for  $\omega_J$  of  $1500 \text{ cm}^{-1}$ , (c) simulation of the superconducting state adopting the BCS value for  $\omega_J$  of  $200 \text{ cm}^{-1}$ , (d) *idem.* with a residual Drude conductivity of  $3 \text{ S/cm}$  added close to the plasma resonance. In (b), (c), and (d)  $\sigma_e$  was set to  $0.5 \text{ S/cm}$  near the dominant phonon frequencies.

position of the three longitudinal optical phonons at  $155$ ,  $430$ , and  $630 \text{ cm}^{-1}$ . The solid curve in Fig. 4(b) represents a simulation of the superconducting state adopting  $\omega_J = 1500 \text{ cm}^{-1}$  implied by the ILT model [Eq. (1)], while keeping all other  $c$ -axis parameters unaltered. The three peaks are now of mixed phonon-plasmon character. The large value of the Josephson plasma frequency results in a considerable shift of the two peaks at  $430$  and  $630 \text{ cm}^{-1}$  towards lower frequencies, and a strong suppression of intensity of the  $155 \text{ cm}^{-1}$  mode. The peak at  $700 \text{ cm}^{-1}$  is essentially a screened superfluid plasmon.

Experimentally no Josephson plasmon is observable in Figs. 2 or 4(a) or for the film in Fig. 3 except perhaps for a rather broad feature around  $40 \text{ cm}^{-1}$  in Fig. 3. Taken together with the fact that there is no observable shift of the LO phonons at  $146$ ,  $379$ , and  $594 \text{ cm}^{-1}$  as the temperature is reduced from  $300$  to  $6 \text{ K}$ , an upper limit can be set for the screened plasma resonance of  $40 \text{ cm}^{-1}$ . Using the fitted phonon parameters and  $\epsilon_\infty$  for  $\vec{E} \parallel \vec{c}$ ,<sup>12</sup> this implies that the unscreened Josephson plasma frequency satisfies  $\omega_J < 100 \text{ cm}^{-1}$ , or equivalently the  $c$ -axis penetration depth satisfies  $\lambda_c > 15 \mu\text{m}$  for  $T \rightarrow 0$ . For  $\text{La}_{2-x}\text{Sr}_x\text{CuO}_4$  and  $\text{Tl}_2\text{Ba}_2\text{CuO}_6$  the fraction of the condensation energy contributed by the ILT mechanism  $\eta = (\omega_J^{\text{exp}}/\omega_J^{\text{ILT}})^2 \approx 0.2$  and  $\eta < 0.005$ , respectively.  $\text{Tl}_2\text{Ba}_2\text{CuO}_6$  differs from  $\text{La}_{2-x}\text{Sr}_x\text{CuO}_4$  in other respects: The very low normal-state  $c$ -axis conductivity ( $< 2 \text{ S/cm}$  at  $100 \text{ K}$ ) combined with a linear rise as a function of temperature has been noticed before and is confirmed both from our dc measurements and from the dynamical conductivity around  $500 \text{ cm}^{-1}$  obtained

from our analyses of the line shape of the prominent longitudinal optical phonons. These observations, and the very low  $c$ -axis Josephson plasma frequency definitely pose a challenge both to “conventional” mechanisms and to the implementation of the ILT model as it was described in Ref. 1. To comply with these facts within the context of an ILT mechanism one may postulate<sup>18</sup> the existence of small electron pockets in the TIO layers, which are also two-dimensional (2D) and cross the main CuO band only at a few points in 2D  $k$  space. The matrix element which would un-cross these bands is then restricted in 2D  $k$  space, which leads to a reduced value of  $\omega_j^2$ , while  $T_c$  depends mainly on those parts of Fermi surface where the crossing occurs. Within this scenario large portions of the Fermi surface should exist where  $|\Delta| \ll |\Delta_{\max}|$ , which can be tested experimentally.

We measured the  $c$ -axis infrared properties of thin platelike  $\text{Tl}_2\text{Ba}_2\text{CuO}_6$  single crystals and thin films and the

$ab$  face of  $\text{La}_{2-x}\text{Sr}_x\text{CuO}_4$  using grazing incidence infrared spectroscopy. The screened plasma resonance of  $\text{Tl}_2\text{Ba}_2\text{CuO}_6$  was found to be below  $40 \text{ cm}^{-1}$ , corresponding to an unscreened  $c$ -axis Josephson plasma frequency of  $100 \text{ cm}^{-1}$  and a lower limit of the  $c$ -axis penetration depth of  $15 \mu\text{m}$ . These experimental results, together with the low value of the conductivity along the  $c$  direction, pose a challenge both to conventional theories and the interlayer tunneling mechanism.

D.v.d.M gratefully acknowledges numerous fruitful discussions with P.W. Anderson and A.J. Leggett at various stages of this project. This investigation was supported by the Netherlands Foundation for Fundamental Research on Matter (FOM) with financial aid from the Nederlandse Organisatie voor Wetenschappelijk Onderzoek (NWO) and by the EEC (Human Capital and Mobility). The work performed at SUNY/Buffalo was supported by NYSERDA, ORNL, ANL, ONR, and NSF.

\*On leave from P.N. Lebedev Physical Institute, Russian Academy of Sciences, Moscow, 117924 Russia.

<sup>1</sup>S. Chakravarty and P.W. Anderson, Phys. Rev. Lett. **72**, 3859 (1994).

<sup>2</sup>P.W. Anderson, Science **268**, 1154 (1995).

<sup>3</sup>D. van der Marel *et al.*, in *Proceedings of the 10th Anniversary HTS Workshop on Physics, Materials and Applications*, Houston, Texas, edited by B. Batlogg, C. W. Chu, W. K. Chu, D. U. Gubser, and K. A. Müller (World Scientific, Singapore, 1996), pp. 357–360.

<sup>4</sup>A.J. Leggett, Science **274**, 587 (1996).

<sup>5</sup>J. Loram (private communication).

<sup>6</sup>M. Tinkham, *Introduction to Superconductivity* (McGraw-Hill, New York, 1996).

<sup>7</sup>N. N. Kolesnikov *et al.*, Physica C **242**, 385 (1995).

<sup>8</sup>H.M. Duan *et al.*, Physica C **185**, 1283 (1990); T. Manako *et al.*, *ibid.* **185**, 1327 (1990).

<sup>9</sup>C. A. Wang *et al.*, Physica C **262**, 98 (1996).

<sup>10</sup>H.S. Somal *et al.*, Phys. Rev. Lett. **76**, 1525 (1996).

<sup>11</sup>O.K.C. Tsui, N.P. Ong, and J.B. Peterson, Phys. Rev. Lett. **76**, 819 (1996).

<sup>12</sup>Using Eq. (3) the fit parameters of the phonons are  $\epsilon_\infty = 4.0$  and  $\{\omega_{T_j}(\text{cm}^{-1}), S_{j,1}/\tau_j(\text{cm}^{-1})\} = \{146, 0.30, 1\}, \{379, 0.93, 8\}, \{594, 0.31, 8\}$  ( $j = 1 \dots 3$ ).

<sup>13</sup>A.D. Kulkarni *et al.*, Phys. Rev. B **41**, 6409 (1990).

<sup>14</sup>Jae H. Kim *et al.*, Phys. Rev. B **49**, 13 065 (1994).

<sup>15</sup>A.V. Puchkov *et al.*, Phys. Rev. B **51**, 3312 (1990).

<sup>16</sup>K. Tamasaku, Y. Nakamura, and S. Uchida, Phys. Rev. Lett. **69**, 1455 (1992).

<sup>17</sup>J. H. Kim *et al.*, Physica C **247**, 297 (1995).

<sup>18</sup>P.W. Anderson (private communication).